Journal of The Electrochemical Society, **156** (8) H640-H643 (2009)
0013-4651/2009/156(8)/H640/4/$25.00 © The Electrochemical Society

Effects of Laser Sources on Damage Mechanisms and Reverse-Bias Leakages of Laser Lift-Off GaN-Based LEDs

Ji-Hao Cheng,[a,*] YewChung Sermon Wu,[a,,z] Wei Chih Peng,[a] and Hao Ouyang[b]**

[a]*Department of Materials Science and Engineering, National Chiao Tung University, Hsinchu 300, Taiwan*
[b]*Department of Materials Engineering, National Tsing Hua University, Hsinchu 300, Taiwan*

The frequency-tripled neodymium-doped yttrium aluminum garnet laser (355 nm) and the KrF pulsed excimer laser (248 nm) were employed to separate GaN thin films from sapphire substrates and to transfer the films to bond with other substrates. The different laser lift-off processes would generate the dislocation density on different regions. In this study, the effects of these two laser sources on structural damage mechanisms and reverse-bias leakages of InGaN–GaN light-emitting diodes (LEDs) were studied.
© 2009 The Electrochemical Society. [DOI: 10.1149/1.3148251] All rights reserved.

Manuscript submitted April 3, 2009; revised manuscript received May 4, 2009. Published June 12, 2009.

Light-emitting diodes (LEDs) are expected to play the most important role in next-generation light source due to their advantages of long life, high efficiency, small size, various colors, and wide applications. In particular, the high brightness GaN-based LEDs have attracted considerable attention for white light solid-state lighting. GaN-based LEDs usually were grown on sapphire and have improved quickly due to rapid advances in growth techniques. However, owing to the poor thermal and electrical conductivity of sapphire substrate, which affects the LED efficiency and reliability, the GaN layer usually has a high defect density.

The current progress may be further extended by combining the GaN-based LEDs with other materials such as Si, Cu, and diamond. A less direct integration method involves laser lift-off (LLO) and transfer for bonding with dissimilar materials.[1-3] Several laser sources including the frequency-tripled neodymium-doped yttrium aluminum garnet (Nd:YAG) laser (355 nm)[4,5] and the KrF pulsed excimer laser (248 nm) have been demonstrated to successfully separate GaN thin films from sapphire substrates.[6] During laser scanning, the GaN layer will decompose into Ga metal and nitrogen gas. Consequently, the freestanding GaN layer is separated from the sapphire. These LLO processes would degrade the performance of InGaN–GaN LEDs. In this study, the effect of these two laser sources on the defect generation mechanisms and reverse-bias leakages of InGaN–GaN LEDs was studied.

Experimental

In this study, three types of LEDs were investigated. Samples designated as "CV-LED" were conventional LEDs without any laser treatment. Samples designated as "KrF-LED" were CV-LEDs treated with KrF pulsed excimer laser, while "YAG-LEDs" were CV-LEDs treated with Nd:YAG laser. The basic fabrication processes of these LEDs were almost the same.[7] The LED structures were grown by low pressure metallorganic chemical vapor deposition. The structures comprised a 5 nm thick Si-doped n^+-InGaN layer, a 400 nm thick Mg-doped p-GaN layer, an InGaN–GaN multiple quantum well (MQW), a 2 μm thick Si-doped n-GaN layer, a 2 μm thick undoped-GaN layer film, and a buffer layer on the sapphire substrate.

For the CV-LED, the device mesa with a chip size of 350 × 350 μm was defined by an inductively coupled plasma which removed the Mg-doped GaN and MQW until the Si-doped GaN was exposed. Then, the indium tin oxide (ITO) layer was deposited on the n^+-InGaN layer using an E-beam coater to form a p-side contact layer and a current spreading layer. The Cr/Au layer was deposited onto the ITO layer to form the p- and n-side electrodes.

The fabrication processes of KrF-LED and YAG-LED are shown in Fig. 1. Before the LLO process, the CV-LED wafer was bonded to a host substrate covered with an adhesive/glue layer, and the sapphire substrate of KrF-LED was polished using a diamond paper. The KrF laser beam spot size of 700 × 700 μm (four chips were lifted off in etch pulse) was scanned without overlap from pulse to pulse. The 355 nm Nd:YAG LLO system was constructed by a series of lens, the laser beam was near circle shape, and the lateral energy of the converged laser beam was a Gaussian distribution. The Nd:YAG laser beam spot size of 500 μm was scanned with a 20% overlap from pulse to pulse.

The pulse length of the KrF laser was 35 ns, which was longer than that of the YAG laser (5 ns). The energy densities of the KrF laser were in the range between 700 and 1000 mJ/cm^2, while those of the YAG laser were in the range between 100 and 400 mJ. These wafers were then bonded to a sapphire substrate with an adhesive layer at 200°C for 60 min with a comprehensive load of 10 kg/cm^2. The host substrate and glue layer were subsequently removed.

Results and Discussion

After LLO, for KrF-LED, when the laser energy was below 700 mJ/cm^2, no visible alteration of the GaN layer was observed.

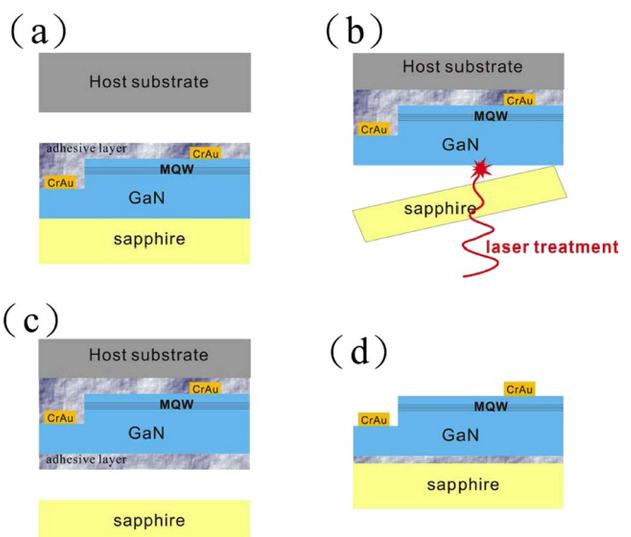

Figure 1. (Color online) Schematic diagram of YAG-LED and KrF-LED transfer process: (a) CV-LED bonding to host substrate, (b) LLO process, (c) bonding to sapphire substrate, and (d) removal of host substrate and glue layer.

* Electrochemical Society Student Member.
** Electrochemical Society Active Member.
z E-mail: sermonwu@stanfordalumni.org

Downloaded on 2014-04-25 to IP 140.113.38.11 address. Redistribution subject to ECS terms of use (see ecsdl.org/site/terms_use) unless CC License in place (see abstract).

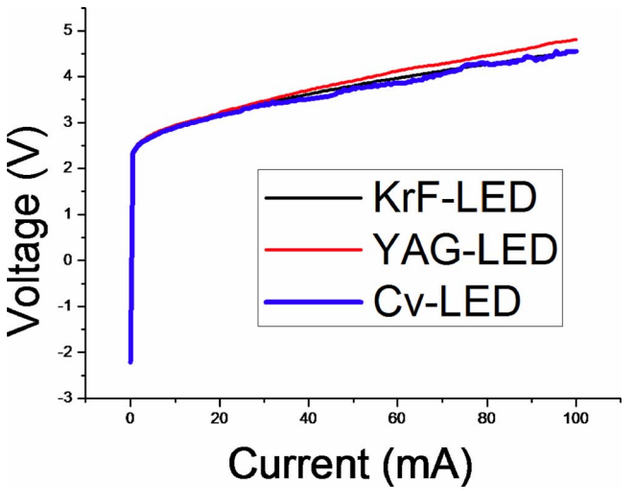

Figure 2. (Color online) *I-V* curve of forward voltage characteristics of KrF-LED, YAG-LED, and CV-LED.

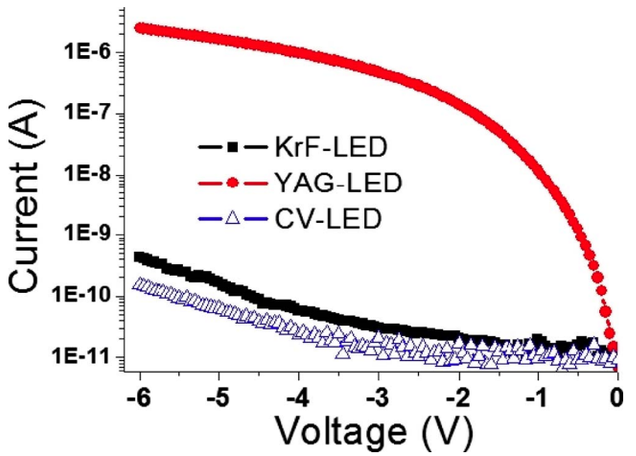

Figure 3. (Color online) Leakage currents of LEDs under a reverse bias of −5 V.

The GaN layers were lifted off when the laser intensity was above this critical energy. However, when the laser energy exceeded 900 mJ/cm^2, the absorbed photon energy led to local heating of the layer above the critical sublimation temperature of Ga, causing the destruction of the GaN layer. As a result, most LED devices failed after such high energy laser treatment.[7] Only those devices with a median energy density (800 mJ/cm^2) had good yields ($>$ 90 %). As for YAG-LED, the median energy density of the YAG laser was 200 mJ/cm^2.[7] These two laser energy intensities were utilized to study the effects of various laser sources on the damage mechanisms and reverse-bias leakages of LEDs.

Figure 2 shows the current–voltage (*I-V*) characteristics of the LEDs. The forward voltages of both KrF-LED and YAG-LED were about 3.2 V at 20 mA, which was similar to that of CV-LED (3.2 V), indicating that the transfer method did not change the LED performance much. The light intensity of CV-LED was 96 mcd (at 20 mA), which was larger than the KrF-LED (84 mcd) and YAG-LED (81 mcd). This is because, when the light passes through the bonded interface, the Fresnel losses resulting from the GaN/adhesive layer and adhesive layer/sapphire interfaces might have a negative effect on the luminance intensity. Besides, during the bonding process, we might create interfacial defects at the bonded interface. These defects have a negative effect on the optical properties.

However, the reverse-bias leakage currents of three LEDs were quite different. Figure 3 shows the reverse-bias leakage currents of LEDs up to −5 V. Leakage currents increased with laser energy densities. Under a reverse bias of −5 V, the leakage current of YAG-LED was 1.65 $\times$ 10^3 nA, which was 10,000 times higher than that of the KrF-LED (0.17 nA) and 33,000 times higher than that of the CV-LED (0.05 nA). Because these LED devices were fabricated from the same wafer, these degradations must be caused by the LLO processes, which generated screw dislocations. These dislocations had been demonstrated as the primary culprit in reverse-bias leakage paths in GaN.[8-12]

A transmission electron microscopy (TEM) image with a two-beam condition was employed to identify screw dislocations. The low loss region of transmission electron-energy-loss spectroscopy was utilized to estimate the sample thickness to obtain accurate dislocation density.[13] The distribution of dislocation densities of these two lift-off LEDs was quite different. Figure 4 shows the cross-sectional TEM images of LEDs. Figure 4 shows the cross-sectional TEM images of LEDs with a (0002) two-beam condition to observe the screw dislocation. The dislocation densities were obtained by counting the number of dislocations and then dividing it by the thickness and width of TEM sampling regions. In this case, those dislocations that penetrated through the MQW region were counted because they could affect the leakage current of the LED. The screw dislocation density in the MQW region of YAG-LED (2.9 $\times$ 10^9 cm^{-2}) was much higher than that of KrF-LED (3.75 $\times$ 10^8 cm^{-2}). Therefore, the reverse-bias leakage current of YAG-LED was higher than that of KrF-LED.

Figures 5a and 6a show the enlarged superficial region of YAG-LED and KrF-LED, respectively. The dislocation density near the LLO surface of KrF-LED was higher than that of YAG-LED. Their relative dislocation densities were schematically illustrated in Fig. 7. The MQW dislocation density of KrF-LED was lower than that of YAG-LED. The LLO surface dislocation density of KrF-LED was higher than that of YAG-LED.

The difference in dislocation densities of the two LEDs in the MQW region is because the absorption coefficient of GaN at 248 nm (for KrF-LED) is 2 $\times$ 10^5 cm^{-1}, which is 3.33 times higher than that at 355 nm (for YAG-LED) (6 $\times$ 10^4 cm^{-1}).[14] In other words, the absorption depth of the YAG laser was much thicker than that of the KrF excimer laser. The absorption of laser energy induces a highly localized, rapid, thermal decomposition of GaN. This decomposition which introduces a biaxial compressive stress can cause deformation (formation of dislocations) of the GaN layer. Compared to the KrF excimer laser, the YAG laser had a thicker absorption depth, which causes more dislocations to be formed in the MQW region, resulting in an increase in reverse-bias leakage current.

Besides dislocations, serious stacking faults were observed within approximately 40 nm of the LLO interface, as shown in Fig. 5b and 6b. The detailed analysis was displayed in Fig. 5c and d, 6c, and d, which show the computed fast Fourier transforms taken from different parts of Fig. 5b and 6b indicated by the arrows. Figures 5d and 6d show regular diffraction spots indicating good crystal quality. In Fig. 5c and 6c, the (0001) and (000$\bar{1}$) spots were pulled into lines toward the center spot, meaning the existence of a huge amount of stacking faults. Besides, some twin spots were also observed in this region. The presence of the stacking faults at the same distance indicates the occurrence of LLO at the GaN/sapphire interface for both KrF and YAG laser sources.[15,16]

Figures 5e and 6e show the enlargement of the part of the lattice image approximately 200 nm below the LLO surface. Figure 5e (YAG-LED) shows a regular lattice image, while Fig. 6e (KrF-LED) shows a distorted image. There are obviously different microstructures at 200 nm below the LLO surface; therefore, the inverse fast Fourier transform (IFFT) was adopted to further analyze this region. They were analyzed by IFFT. Figure 6g displays the processed IFFT image of Fig. 6f (200 nm below the LLO surface of KrF-LED)

Downloaded on 2014-04-25 to IP 140.113.38.11 address. Redistribution subject to ECS terms of use (see ecsdl.org/site/terms_use) unless CC License in place (see abstract).

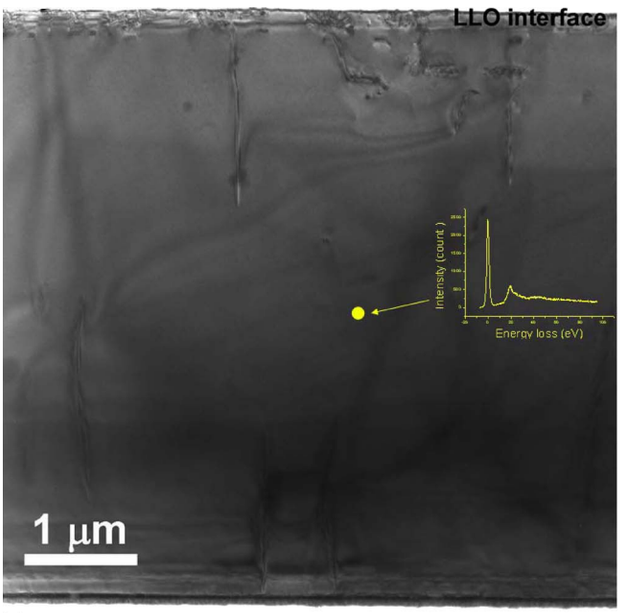

(a)

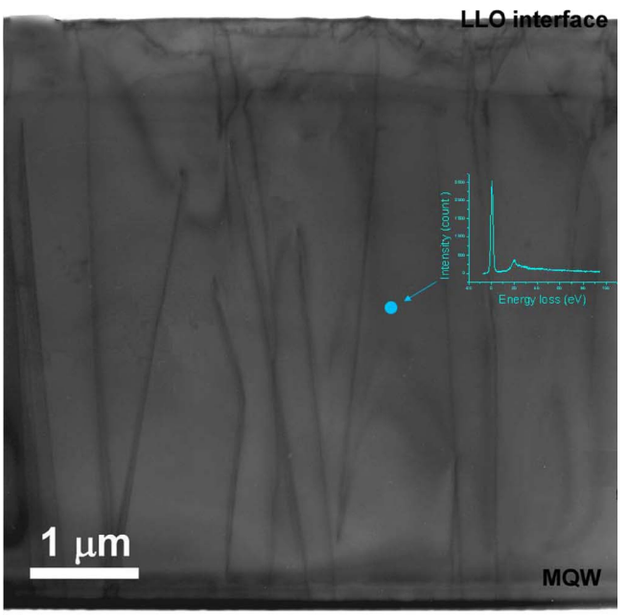

(b)

Figure 4. (Color online) TEM images of the whole LED structure: (a) KrF-LED and (b) YAG-LED.

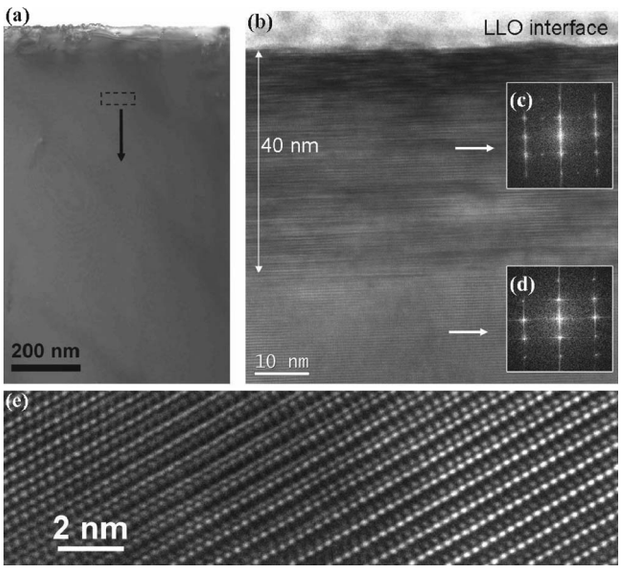

Figure 5. TEM images of YAG-LED: (a) bright-field cross-sectional image of the YAG-LED LLO interface, (b) magnified part of the superficial region from (a), [(c) and (d)] fast Fourier transforms of different regions indicated by arrows, and (e) HRTEM lattice image of the region 200 nm below the LLO interface.

using the diffraction spots along the [0002] direction. KrF-LED has sequential series dislocations, which have the same center, indicated by the dashed white arc lines. The processed IFFT image of YAG-LED did not show such series dislocations.

Similar results have been reported by Chen et al.[16] who analyzed GaN LLO surfaces using a single KrF excimer laser pulse with an energy density of 600 mJ/cm^2. GaN surface regions were characterized by cross-sectional high resolution transmission electron microscopy (HRTEM) and fitted using the model of stress waves. They found, in addition to the superficial damages caused by laser absorption, a cluster of half-loops (sequential series dislocations) near the LLO interface, which were generated by a laser-induced shock wave. The stress wave model analysis revealed that when the pulse duration exceeded the critical time (10 ns), plastic waves were generated and converged at a position accompanied by stress saltation. The shock-wave-generating position was about 200 nm away from the LLO surface.

In our study, because the KrF-laser pulse time (35 ns) was longer than the critical time, a cluster of half-loops was also found at about 200 nm away from the LLO surface (Fig. 5c). However, no loops were found near the LLO surface of YAG-LED because the pulse time (5 ns) was shorter than the critical time. As a result, the screw dislocation density near the LLO surface of KrF-LED was higher than that of YAG-LED.

The TEM observation and the effect of absorption constant are summarized in Fig. 7. Compared to YAG laser, KrF excimer laser had a higher absorption coefficient of GaN (shallower penetration depth). Most KrF laser energy was absorbed around the GaN/sapphire interface. However, the longer pulse time brought about plastic and shock wave, which caused the dense dislocation and deformed the superficial structure. As for YAG-LED, owing to the lower absorption coefficient, the Nd:YAG laser had deeper penetration depth, which caused more dislocations in the bulk region and penetrated the MQW region (Fig. 4b) and led to an increase in reverse-bias leakage current.

Conclusion

In this study, the effects of the frequency-tripled Nd:YAG laser (355 nm) and the KrF pulsed excimer laser (248 nm) on the structural damage mechanisms and reverse-bias leakages of GaN-based LEDs were investigated. The absorption depth of the YAG laser was much thicker than that of the KrF excimer laser because the absorption coefficient of GaN at 248 nm is 3.33 times higher than that at 355 nm. As a result, the MQW screw dislocation density and the reverse-bias leakage current of YAG-LED were much higher than those of KrF-LED. Most KrF laser energy was absorbed around the GaN/sapphire interface. Consequently, the LLO surface dislocation density of KrF-LED was higher than that of YAG-LED. Moreover, the longer pulse time of the KrF laser (35 ns) brought about plastic and shock waves, which caused dense dislocation and deformed the superficial structure.

Downloaded on 2014-04-25 to IP 140.113.38.11 address. Redistribution subject to ECS terms of use (see ecsdl.org/site/terms_use) unless CC License in place (see abstract).

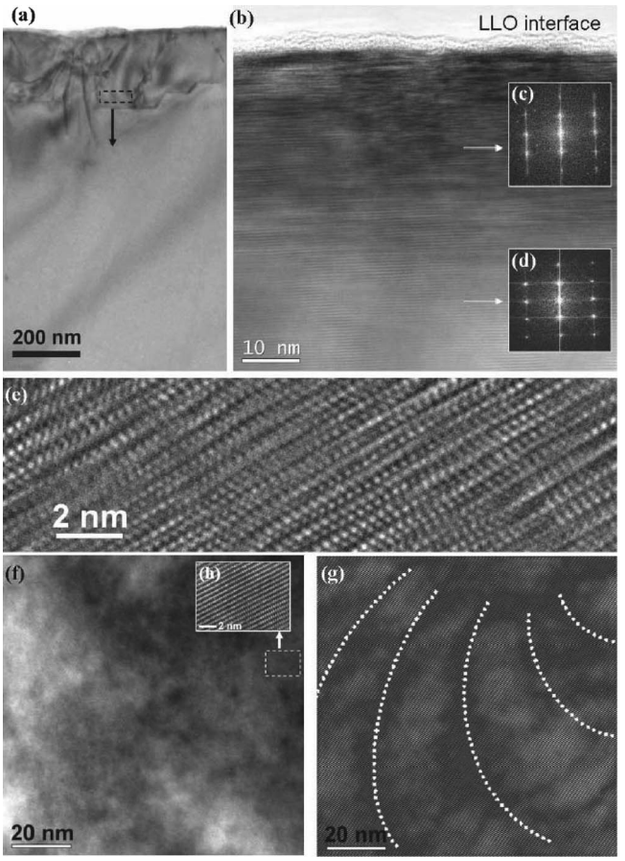

Figure 6. TEM images of the KrF-LED: (a) bright-field cross-sectional image of the KrF-LED LLO interface, (b) magnified part of the superficial region from (a), [(c) and (d)] fast Fourier transforms of different regions indicated by arrows, (e) HRTEM lattice image of the region 200 nm below the LLO interface, (f) TEM image of the region 200 nm from (a), (g) inversed fast Fourier transform image of (f) using diffraction spots along the [0002] direction, and (h) HRTEM lattice image of the region indicated by arrow.

Acknowledgment

This project was funded by Epistar Corporation, Sino American Silicon Products Incorporation, and the National Science Council of the Republic of China under grant no. 95-2221-E009-087-MY3. Technical support from the National Nano Device Laboratory, Center for Nano Science and Technology, Nano Facility Center, and Semiconductor Laser Technology Laboratory of the National Chiao Tung University is also acknowledged. The authors thank H. C. Kuo for valuable discussions.

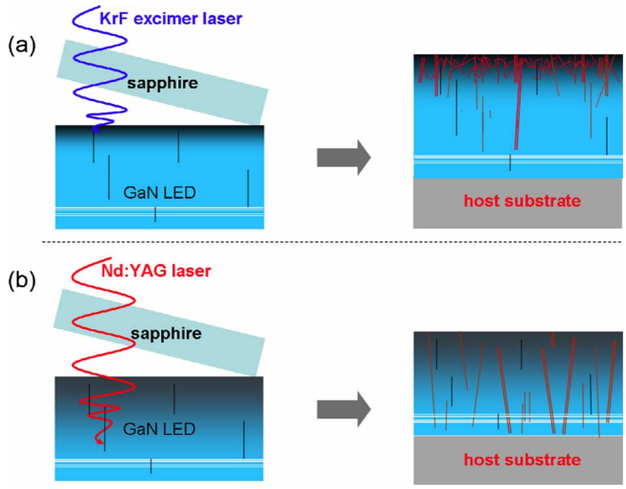

Figure 7. (Color online) Schematic diagram of screw dislocation generation after the lift-off process.

National Chaio Tung University assisted in meeting the publication costs of this article.

References

1. W. Y. Lin, D. S. Wuu, K. F. Pan, S. H. Huang, C. E. Lee, W. K. Wang, S. C. Hsu, Y. Y. Su, S. Y. Huang, and R. H. Horng, *IEEE Photonics Technol. Lett.*, **17**, 1809 (2005).
2. O. B. Shchekin, J. E. Epler, T. A. Trottier, T. Margalith, D. A. Steigerwald, M. O. Holcomb, P. S. Martin, and M. R. Krames, *Appl. Phys. Lett.*, **89**, 071109 (2006).
3. M. R. Krames, O. B. Shchekin, R. Mueller-Mach, G. O. Mueller, L. Zhou, G. Harbers, and M. G. Craford, *J. Disp. Technol.*, **3**, 160 (2007).
4. W. C. Peng and Y. S. Wu, *Appl. Phys. Lett.*, **88**, 181117 (2006).
5. M. K. Kelly, O. Ambacher, R. Dimitrov, R. Handschuh, and M. Stutzmann, *Phys. Status Solidi A*, **159**, R3 (1997).
6. W. S. Wong, T. Sands, and N. W. Cheung, *Appl. Phys. Lett.*, **72**, 599 (1998).
7. Y. S. Wu, J. H. Cheng, W. C. Peng, and H. Ouyang, *Appl. Phys. Lett.*, **90**, 251110 (2007).
8. P. Kozodoy, J. P. Ibbetson, H. Marchand, P. T. Fini, S. Keller, J. S. Speck, S. P. DenBaars, and U. K. Mishra, *Appl. Phys. Lett.*, **73**, 975 (1998).
9. J. W. P. Hsu, M. J. Manfra, D. V. Lang, S. Richter, S. N. G. Chu, A. M. Sergent, R. N. Kleiman, L. N. Pfeiffer, and R. J. Molnar, *Appl. Phys. Lett.*, **78**, 1685 (2001).
10. D. S. Li, H. Chen, H. B. Yu, H. Q. Jia, Q. Huang, and J. M. Zhou, *J. Appl. Phys.*, **96**, 1111 (2004).
11. J. W. P. Hsu, M. J. Manfra, R. J. Molnar, B. Heying, and J. S. Speck, *Appl. Phys. Lett.*, **81**, 79 (2002).
12. B. S. Simpkins, E. T. Yu, P. Waltereit, and J. S. Speck, *J. Appl. Phys.*, **946**, 1448 (2003).
13. R. F. Egerton, *Electron Energy-Loss Spectroscopy in the Electron Microscope*, 2nd ed., Plenum, New York (1996).
14. J. F. Muth, J. H. Lee, I. K. Shmagin, R. M. Kolbas, H. C. Casey, Jr., B. P. Keller, U. K. Mishra, and S. P. DenBaars, *Appl. Phys. Lett.*, **71**, 18 (1997).
15. E. A. Stach, M. Kelsch, E. C. Nelson, W. S. Wong, T. Sands, and N. W. Cheung, *Appl. Phys. Lett.*, **77**, 1819 (2000).
16. W. H. Chen, X. N. Kang, X. D. Hu, R. Lee, Y. J. Wang, T. J. Yu, Z. J. Yang, G. Y. Zhang, L. Shan, K. X. Liu, et al., *Appl. Phys. Lett.*, **91**, 121114 (2007).

Downloaded on 2014-04-25 to IP 140.113.38.11 address. Redistribution subject to ECS terms of use (see ecsdl.org/site/terms_use) unless CC License in place (see abstract).